EUROPEAN ORGANIZATION FOR NUCLEAR RESEARCH
Laboratory for Particle Physics

Divisional Report **CERN LHC/2002-4 (MMS)**

High Precision Displacement Measurement Using Fiber Optics

G. Berkovic [1], S. Rotter[1], W. Scandale [2], E. Shafir[1] and E. Todesco[2]

We describe laboratory experiments with a fiber-optic sensor employing a chirped laser that detects, with 20-30 micrometer accuracy, displacements of a remote reflective target at distance of 200-500 mm. The requirements of chirp linearity and laser coherence in order to achieve this sensitivity are elaborated. This sensor can be employed for remotely sensing minute displacements of objects in harsh environments, including cryo-magnets in particle accelerators.

1 Electro-Optics Division, Soreq NRC, Yavne, Israel
2 CERN, LHC Division, Geneva, Switzerland

Submitted to Review of Scientific Instruments

Administrative Secretariat
LHC Division
CERN
CH - 1211 Geneva 23

Geneva, Switzerland
3 May 2002

Introduction

Numerous optical techniques exist for sensing distance or displacements. Radar (lidar) and other range finding techniques measuring the round-trip time-of-flight of a pulsed source are practical for distances ranging from tens of meters up to thousands of kilometers, and are commonplace in everyday applications. For shorter distances other techniques have been applied, including methods using a laser whose frequency (or wavelength) changes with time, either linearly [1-7] or sinusoidally [8-10]. Interference between light reflected from the target and a reference yields the frequency difference between them, which is related to the target distance via the times of flight difference and the frequency chirp rate.

A fiber-optic based measurement system will generally be more adaptable to applications where the target accessibility is restricted due to physical limitations or extreme temperature or pressure conditions. We have previously described [11,12] a fiber-optic sensor with a frequency modulated (chirped) laser source for measuring the distance to a reflective target, as well as its velocity. This sensor exhibited a typical precision on the order of 1% of the absolute distance in laboratory experiments for target distances in the range of 200-500 mm.

The present work shows that this approach can be extended to the case of rapid (few secs) detection of much smaller (< 100 μm) *displacements* of the target at these distances. This capability is attractive in view of the need for remotely sensing minute displacements of cryo-magnets in particle accelerators, such as the Large Hadron Collider (LHC) project at CERN [13].

Principle of Measurement

A laser whose wavelength is linearly chirped in time is launched into a 2*2 fiber coupler, and back reflected signals from the coupler tip(s) and a remote target are fed into a photodetector (see Figure 1). These reflected signals have different round-trip times of flight (TOFs), meaning that signals that arrive simultaneously in the detector arm originated at different times from the laser. Due to the chirping of the laser, these coincident signals are of different frequencies ($\nu_i, \nu_j, ..$), and the frequency differences Δn_{ij} are readily detected as beat frequencies by a FFT spectrum analyzer. For a known linear chirp rate $\frac{dn_l}{dt}$ of the laser frequency, these beat frequencies straightforwardly yield [1-7] the TOF difference, and thus the path length difference, Δx, since $\Delta n = \frac{dn_l}{dt}\Delta t = \frac{dn_l}{dt}\cdot\frac{2\Delta x}{c}$

With reference to Figure 1, it is evident that when *DL* = 0, such as for a standard fiber coupler, the beat frequency between the target and either fiber arm corresponds to the target distance x and thus the actual distance is determined, as described in our earlier paper [11]. In fact, it is simpler and more convenient to use a three port circulator.

In this article, we primarily deal with the case of a 2x2 coupler where *DL* and *x* are approximately balanced for their optical path lengths [13]. The outcome is a much more sensitive probe for small (tens of μm) changes in position (*x*) for constant *DL*. The reasons for the much-increased sensitivity in the 'balanced arms' configuration are discussed below.

The measurement system used in this work, shown in Figure 1, consists of commercially available components. The laser (New Focus 6328) can be tuned over the range 1510-1580 nm at a chirp rate ranging from 0.1 nm/sec to 25 nm/sec. The fiber coupler is derived from a standard 2*2 coupler (Etek) using SFM-28 single mode fibers, with FC connectors. Different fiber lengths in the two output arms are achieved by reflection-free attachment of a patch-cord or pigtail onto one arm. An AR coated lens (Thor F-220FC-C) directly snaps onto the fiber connector and collimates the light to a target mirror. We use an InGaAs photo-detector (New Focus 2011) and an FFT spectrum analyzer (Stanford Research 760). The spectrum analysis is performed over acquisition times of typically 3-8 sec, and can incorporate a digital filter (Hanning or Blackmann-Harris).

The laser used in this study is frequency tuned by altering the cavity length, and as such differs from the semiconductor lasers used by others which were tuned by periodic saw-tooth [1-7] or sinusoidal [8-10] modulation of the current. The large tuning range of this laser allows us to collect data during a single unidirectional scan. As a result, our beat frequency spectra appear as a single peak, instead of the envelope of peaks at discrete harmonics of the modulation frequency [5-7].

Results

A typical measurement is exemplified in Figure 2. In this experiment, the laser is chirped from 1540 – 1544 nm at 0.5 nm/sec ≈ $6.3*10^{10}$ Hz/sec. Thus we expect beat frequencies (n_B) of 0.42 Hz per mm of optical path difference (in air). We used a fiber tip to target mirror distance, x = 360 mm, and an imbalance in the coupler arms DL=250 mm; thus the optical path length of 250 mm fiber (n=1.5) approximately balances the target distance. The full curve in Figure 2a shows the spectrum analyzer output, illustrating a very sharp peak around 8 Hz and a broad peak around 150 Hz. The former corresponds to the path difference between the mirror and the tip of the long coupler (reference) arm, and the latter contains both the path difference between the two fiber tips, and that between the mirror and the tip of the short coupler (probe) arm. This assignment is easily verified when one of the three reflections is selectively removed. The reflection from the reference fiber was eliminated by coating it with an index-matching gel; only the broad 150 Hz peak is then recorded (Figure 2b, dotted curve). By terminating the probe coupler arm with an angled tip (e.g. APC-FC connector) only the sharp peak due to the beating between the mirror and reference arm is observed. (Fig. 2b, full curve; this peak appears at slightly different frequency from that in Fig. 2a because the APC termination shortened the probe arm length).

The reason why the higher beat frequency is much broader than the low frequency beat is explained by the coherence properties of the chirped laser source, as will be demonstrated below. We first illustrate how the sharp peaks of the balanced arms configuration may be utilized to detect minute displacements of the target. In Figure 3 we show results when the mirror is intentionally displaced towards the fiber tip in 100 μm increments. The raw spectrum analyzer data clearly differentiates each position. Note that the analyzer output is actually a histogram of signal weights for frequency 'bins' of 0.122 Hz segments. The location of the peak in the spectrum is therefore discretized, and this limits the resolution in the displacement measurement. Indeed, one can use algorithms to interpolate the spectrum around the peak following the approach presented in Ref. [14]. The maximum of the interpolating function provides a much more accurate result than the peak of the discrete spectrum. When these interpolated beat frequencies are plotted against the target displacement (Figure 4) the experimental points all fall on the best fit line to within a maximum deviation of 30 μm and rms deviation of 20 μm.

The data of Figures 2 and 3 were achieved for the target aligned for optimal back reflection to the fiber (single pass). As we have pointed out earlier [12,13], in this geometry, when the target mirror is somewhat mis-aligned the single pass reflection will be focussed onto the fiber clad and not guided back into the fiber. However, the small amount of light reflected from the fiber tip will undergo a second pass, and be reflected from the target into the fiber core. We similarly show in Figure 5 the raw spectrum analyzer output for an experiment with a slightly mis-aligned target and $DL \approx 250$ mm and $x \approx 180$ mm, i.e. the optical path lengths are essentially balanced for a double-pass to the target ($1.5DL \approx 2x$). The graph again shows clear shifts in the peak of the beat for 100 μm displacements. We again used the interpolation algorithm to obtain a discrete beat frequency, and now achieved 15-20 μm precision between the known displacement and that derived from the beat frequency shift (Figure 6).

The double-pass operation presents two advantages over single pass operation, at the expense of a lower signal-to-noise ratio. (a) Greater tolerance for distortions and tilt of the target. (b) An inherent doubling of the change in the path length, and thus doubling the shift in ν_B, as the target is displaced. Comparison between Figures 4 and 6 suggests that provided the double-pass mode provides a sufficient signal-to-noise, the effect of (b) can lead to a higher precision than in single-pass mode.

We will now explain why the 'balanced arms' beat frequency peak is much sharper than the beat peaks for unbalanced arms (e.g. the peaks in Fig. 2). We present results of measurements without targets – *i.e.* only the interference between reflections from the two fiber tips – as the arm imbalance ΔL is varied. It is seen in Figure 7 that the peaks broaden as the imbalance, and thus the time-of-flight difference, is increased. This phenomenon has been discussed by Uttam and Culshaw [6] in terms of phase noise and coherence time t_{coh} for the scanned laser. The coherence time represents the average

time over which the propagation of the optical phase deviates from its ideal behavior. In the absence of scanning, the coherence time is directly connected to the laser linewidth, whereas during scanning additional factors arising from the mechanical and/or electronic perturbations and mode hopping will contribute. It is evident from Figure 7 that these effects become more probable as the TOF difference increases. The Figure shows that a typical time for peak broadening to occur is of the order of the round trip time in 100 mm fiber, or 1 nsec. Note that this characteristic time (length) for peak broadening appears to decrease further if the laser is chirped at a faster rate, as shown in Figure 8. The figure shows that for a constant *DL*, i.e. a constant time, more broadening is observed as the laser is chirped faster.

The data of Figures 2-5 show that sharp peaks may be obtained for small imbalances (sub nsec TOF differences), relative to the effective coherence length of the scanned laser. The highly linear nature of the laser chirp under these conditions, manifested by the sharp peaks, is further emphasized by Figure 9, which compares the beat frequency measured for chirping the laser at slightly different initial wavelengths and constant wavelength chirp $d\lambda/dt$. This change in λ should slightly alter the frequency chirp $\frac{d\nu}{dt} = \frac{-c}{\lambda^2} \cdot \frac{d\lambda}{dt}$ and thus the beat frequency. The observed beat frequencies indeed follow this λ^{-2} functional dependence (Figure 10).

Thus in a displacement sensing application, faster chirping leads to a larger change of n_B with displacement, which ordinarily implies greater sensitivity. However, our experiments point out several factors which lead to production of broader beat frequency peaks, or otherwise limit the maximum chirp at which accurate displacement may be sensed

- There is a finite range over which the laser may be tuned to give an adequate and fairly constant power output and so the chirp rate (multiplied by acquisition time) should not exceed this range.
- A faster chirp increases the probability of phase noise thus broadening the beat peaks and reducing the resolution.
- The fact that the chirp is linear in $\frac{d\lambda}{dt}$, and not in $\frac{d\nu}{dt}$ also causes increased peak broadening with faster chirp.

In view of these considerations, it is not surprising that our measurements have shown that a chirp rate of around 1 nm/sec (with 8 sec data acquisition time) is optimal for our system.

The authors acknowledge helpful discussions with M. Tur and financial support to the Soreq NRC group via the Israeli Ministry of Trade and Industry's program for Israeli participation in CERN projects.

References

[1] A. Olsson and C.L. Tang, Appl. Opt. **20**, 3503 (1981).

[2] G. Beheim and K. Fritsch, Elect. Lett. **21**, 93 (1985).

[3] G. Beheim and K. Fritsch, Appl. Opt. **25**, 1439 (1986).

[4] U. Minoni, L. Rovati and F. Docchio, Rev. Sci. Instrum. **69**, 3992 (1998).

[5] M. Imai and K. Kawakita Opt. Comm. **78**, 113 (1990).

[6] D. Uttam and B. Culshaw, J. Lightwave Tech. **3**, 971 (1985).

[7] G. Economou, R. C. Youngquist and D.E.N. Davies, J. Lightwave Tech. **4**, 1601 (1986).

[8] H. Kikuta, K. Iwata and R. Nagata, Appl. Opt. **25**, 2976 (1986); Appl. Opt. **26**, 1654 (1987).

[9] A. J. den Boef, Appl. Opt. **26**, 4545 (1987).

[10] E. Fischer, E. Dalhoff, S. Heim, U. Hofbauer and H.J. Tiziani, Appl. Opt. **34**, 5589 (1995).

[11] G. Berkovic and E. Shafir, Proc. SPIE **4185**, 94 (2000)

[12] E. Shafir and G. Berkovic, Meas. Sci. Technol. **12**, 943 (2001).

[13] D. Inaudi, B. Glisic, S. Fakra, J. Billan, J.G. Perez, S. Redaelli and W. Scandale, Meas. Sci. Technol. **12**, 887 (2001).

[14] A. Bazzani, R. Bartolini, M. Giovannozzi, W. Scandale, E. Todesco, Part. Accel. **52**, 147 (1996); also in CERN SL (AP) 95-84.

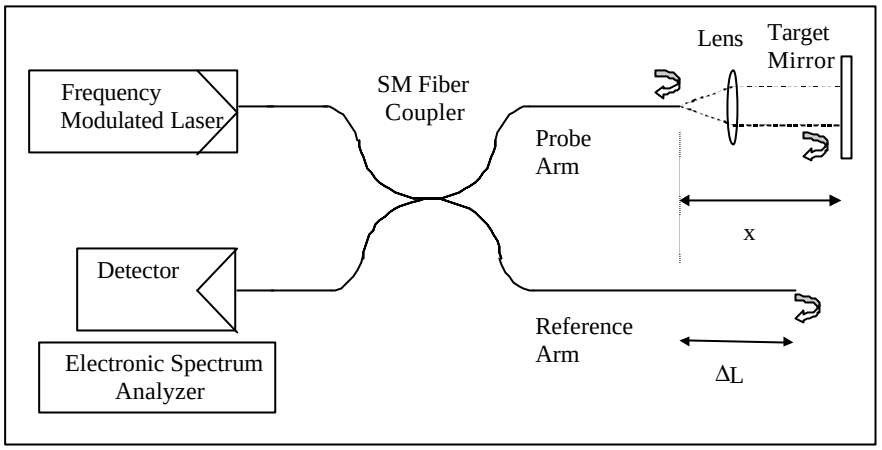

Figure 1. **Experimental set-up showing the three sources of back reflections and the path differences between them.** DL **is the path length between the reference and probe arms of the coupler, and** x **is the distance from the probe arm tip to the reflective target.**

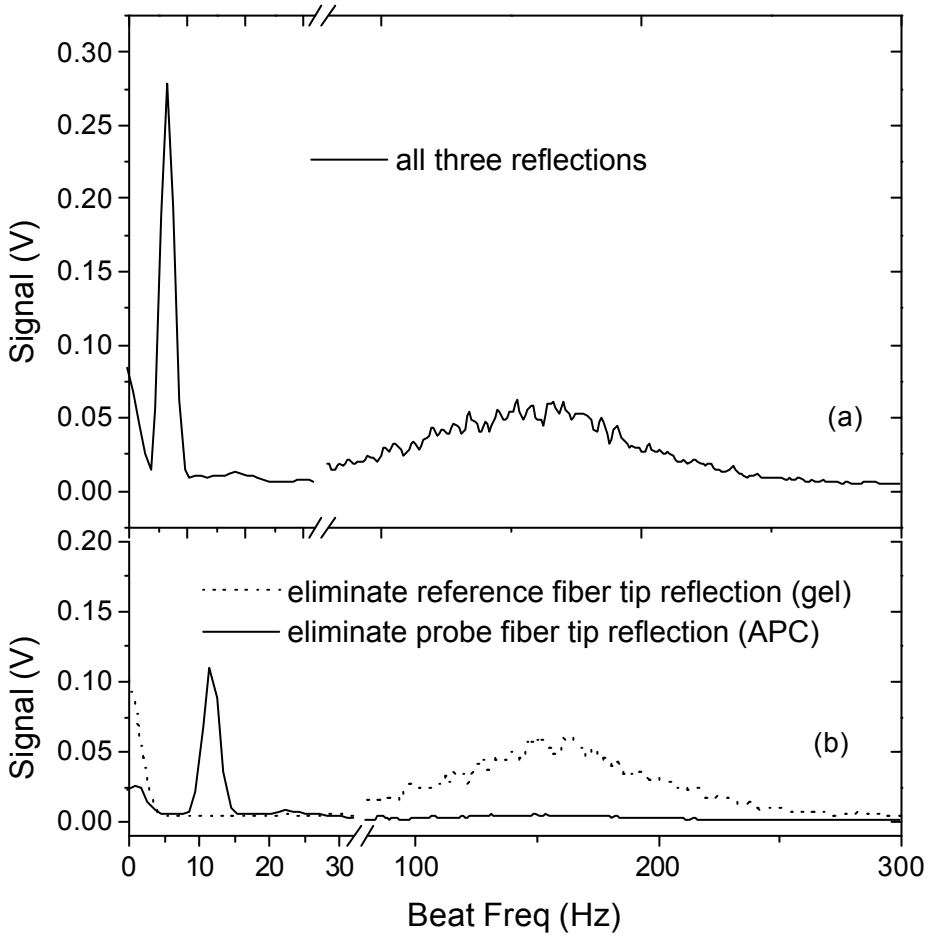

Figure 2. **Beat frequency measurement with** DL **= 250 mm,** x **= 360 mm (according to Figure 1) and 0.5 nm/sec chirp. The top curve shows the result when all three possible reflections – from the two fiber tips and the target – are active. The two curves in the lower graph are obtained when the fiber tip reflection from one coupler arm is eliminated.**

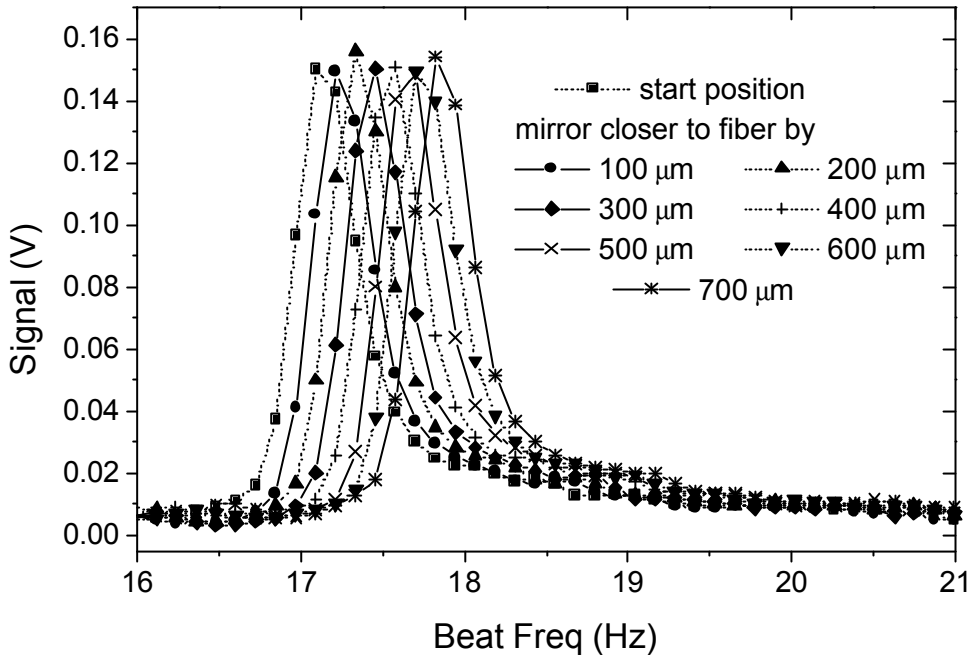

Figure 3. **Detection of 100 μm displacement for target aligned for single pass operation, with DL » 250 mm, x » 360 mm and 1.2 nm/sec chirp.**

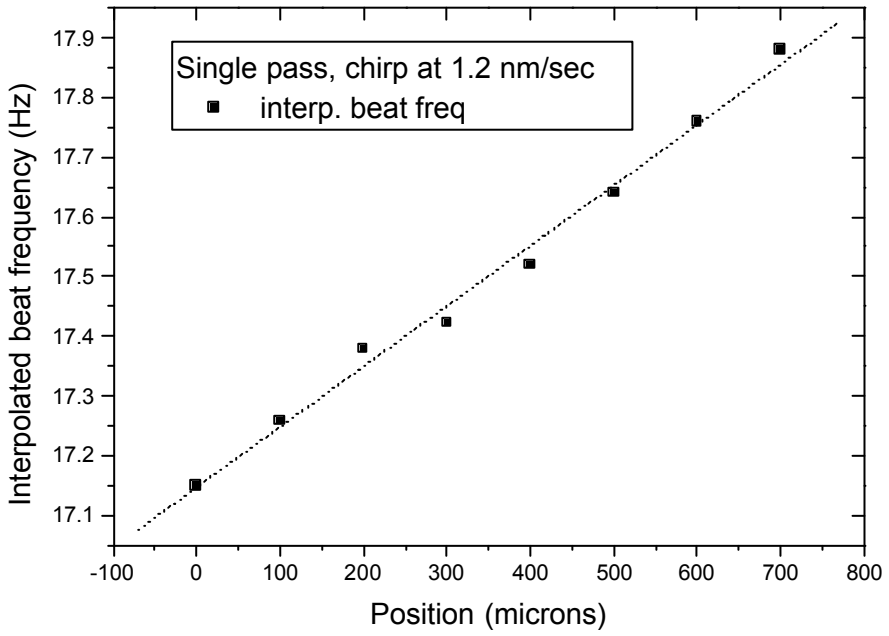

Figure 4. **The best-fit line for the interpolated beat frequency peak for each curve in Fig. 3. The rms deviation of the experimental points from the line is about 20 μm.**

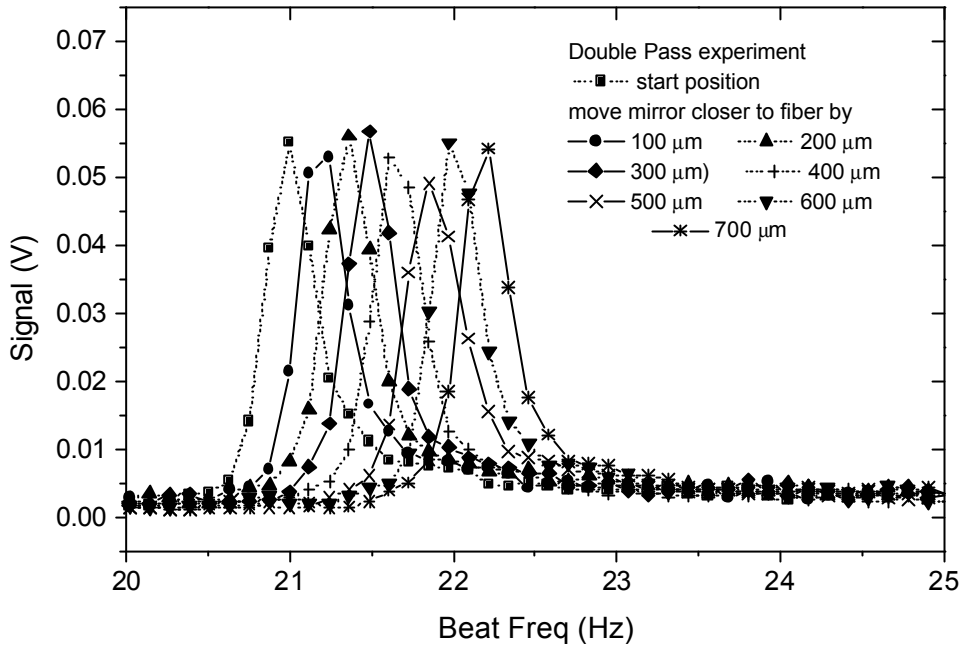

Figure 5 **Detection of 100 μm displacement in double-pass mode for misaligned target, with *DL* » 250 mm, *x* » 175 mm and 1 nm/sec chirp.**

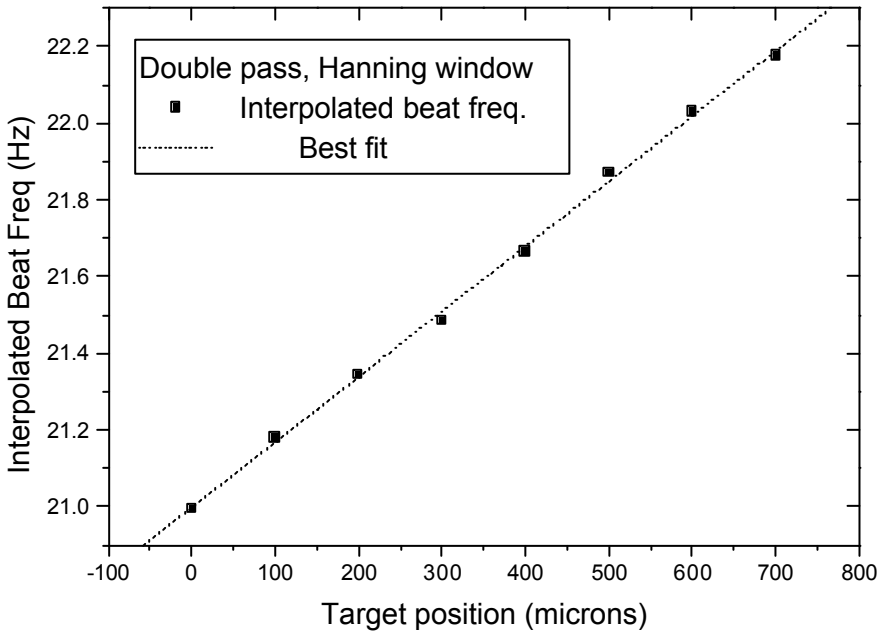

Figure 6**. The best-fit line for the interpolated beat frequency peak for each curve in Fig. 5. The rms deviation of the experimental points from the line is about 15 μm.**

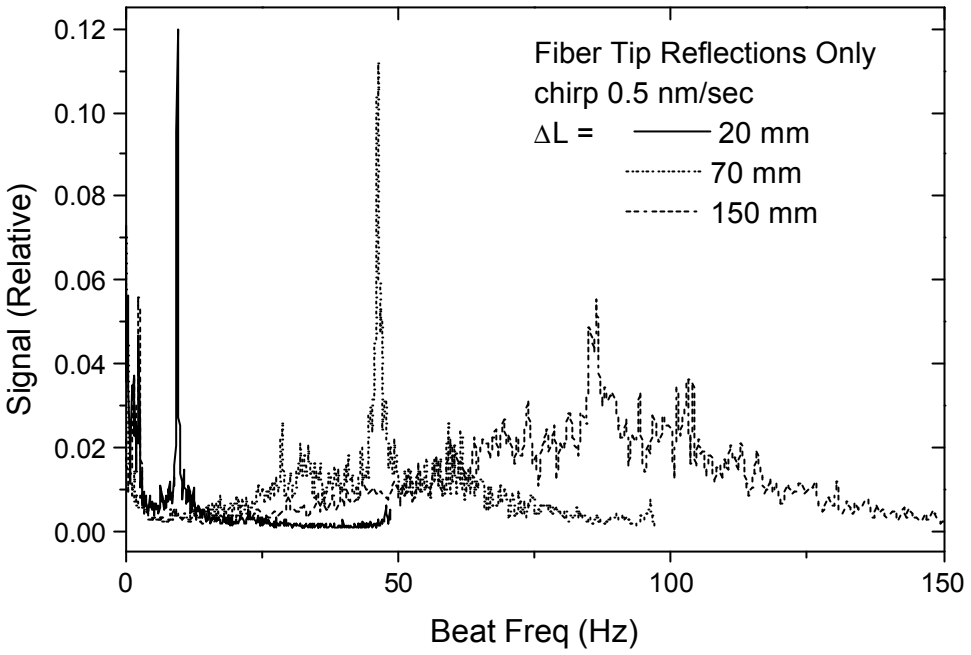

Figure 7 **Broadening of peaks as path length imbalance is increased (for constant chirp rates). The interference is between the back reflections from the two coupler arm tips (no target).**

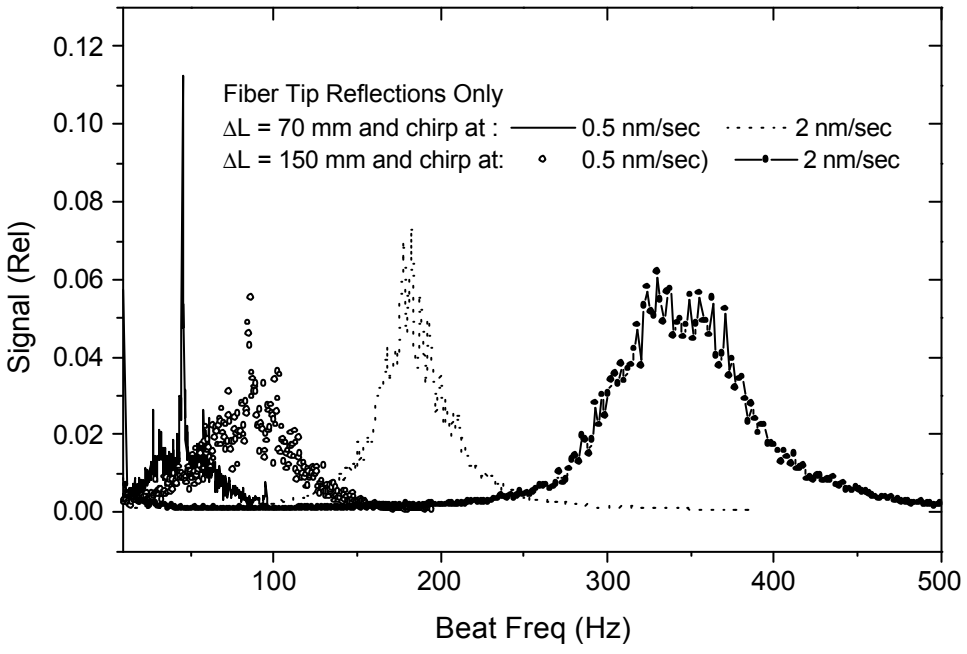

Figure 8 **Broadening of peaks as chirp rate is increased (for two cases of constant imbalance).**

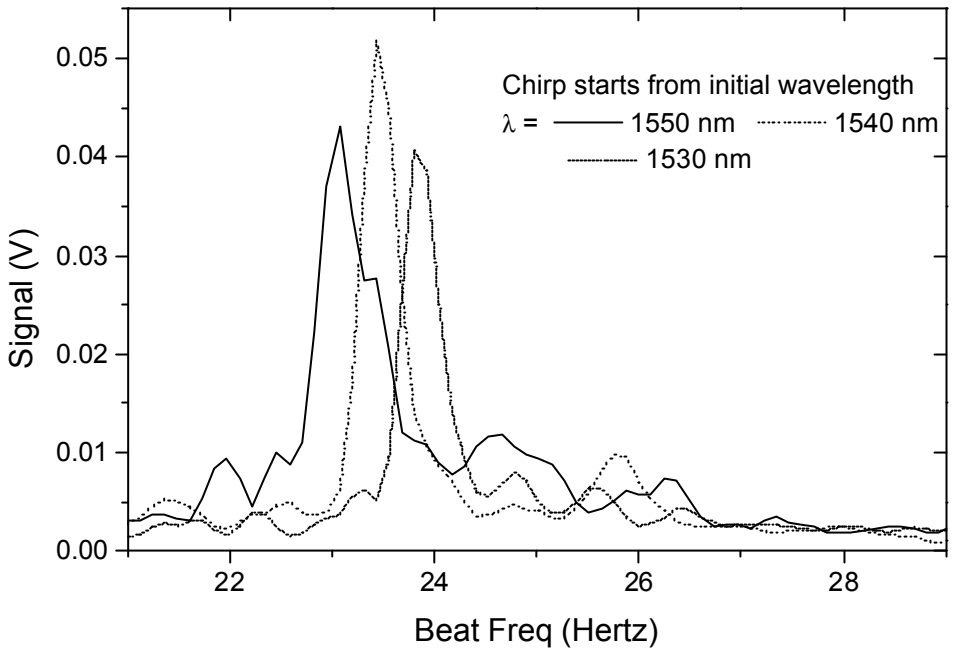

Figure 9 **Experiment demonstrating the *s*hift in n_B with wavelength for chirp at constant dl/dt = 0.7 nm/sec. Each scan took about 8 sec, and started at a different initial l as shown. The measurement is performed in single-pass mode using a mirror at 340 mm from the probe arm tip, such that the distance unbalance to the reference tip was approx. 35 mm.**

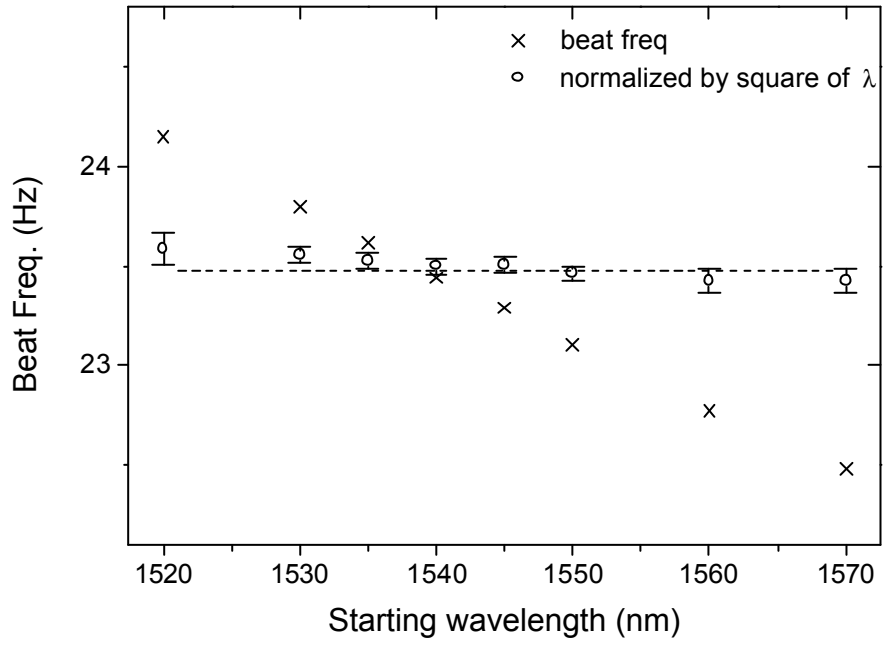

Figure 10 **Plot of the peak n_B values from Figure 9 against the wavelength at the start of the scan (crosses). After dividing by the square of the wavelength at the midpoint of the scan, a constant value is obtained (circles).**